Inorg. Chem. **2007**, *46*, 9513–9515

New Oxalate-Bridged Cr^{III}–Mn^{II} Polymeric Network Incorporating a Spin-Crossover $[Co(terpy)_2]^{2+}$ Cation

Hui-Zhong Kou*,†,‡ and Osamu Sato*,†

Institute for Materials Chemistry and Engineering, Kyushu University, 6-1 Kasuga-koen, Kasuga, Fukuoka 816-8580, Japan, and Department of Chemistry, Tsinghua University, Beijing 100084, People's Republic of China

Received May 29, 2007

The reaction of Mn^{2+} with $[Cr(ox)_3]^{3-}$ in the presence of the spin-crossover $[Co(terpy)_2]^{2+}$ cation gives rise to a 1D $[Co(terpy)_2][Mn(H_2O)ClCr(ox)_3]\cdot H_2O\cdot 0.5MeOH$ (**1**) or a 2D $[Co(terpy)_2][Mn(H_2O)Cr(ox)_3]_2\cdot 5H_2O\cdot 0.5MeOH$ (**2**). The trimetallic complexes display dominant ferromagnetic behavior, and spin-crossover of $[Co(terpy)_2]^{2+}$ is suppressed by the chemical pressure of the polymeric oxalate-bridged network.

Molecule-based magnets derived from two paramagnetic building blocks have been shown to be potentially applied to practical use considering the exciting findings that room-temperature magnets have been achieved.[1] Significantly, the magnetic properties can be tuned and improved by virtue of chemical control and modification. To obtain molecular magnetic materials, it is fundamental to use the bridging ligands that could effectively transmit magnetic coupling. The most popular ligands include cyanide (CN^-), azide (N_3^-), oxalate (ox^{2-}), and oxo (O^{2-} or OH^-). As far as the oxalate-bridged moleculr magnets are concerned, 2D or 3D complexes of the formula $cat[M^{II}M'^{III}(ox)_3]$ ($cat^+ = R_4N^+$, PPh_4^+; M = Mn, Fe, Co, Ni, Cu; M′ = Cr, Fe, Ru) exhibit ferro- or ferrimagnetic ordering with the highest ordering temperature of 44 K.[2] Interestingly, the replacement of the cat^+ cation with conducting bis(ethylenedithio)tetrathiafulvalene (BEDT-TTF or ET) has given rise to the first synthetic ferromagnetic metal,[3a] and when cat^+ is a photochromic N-methylated pyridospiropyran cation (SP^+), the obtained complex $(SP)MnCr(ox)_3\cdot H_2O$ orders ferromagnetically at 5.5 K and exhibits crystalline-state photochromism.[3b]

Some $3d^{4-7}$ transition-metal complexes exhibit magnetic bistability (spin-crossover, SCO) at a certain temperature (T_c) between high-spin and low-spin states and therefore are anticipated to be used as switching devices.[4,5] Encapsulation of the SCO cations in magnetically coupled chains, sheets, or 3D anions might give rise to novel composite magnetic materials that can be used for significant investigations on cooperative (synergic) behavior.[6,7] It is especially interesting to synthesize complexes with two magnetic phase transitions, for example, long-rang magnetic ordering and SCO.[8] To this end, we prepared two novel complexes containing oxalate-bridged $Mn^{II}-Cr^{III}$ polymeric anions and the SCO $[Co(terpy)_2]^{2+}$ cation,[9] which are reported herein.[10] $[Co(terpy)_2](ClO_4)_2$ shows gradual SCO behavior between ^2E ($t_{2g}^6e_g^1$) and $^4T_1$ ($t_{2g}^5e_g^2$) states with a transition temperature

* To whom correspondence should be addressed. E-mail: kouhz@mail.tsinghua.edu.cn (H.-Z.K), sato@chem.kyushu.ac.jp (O.S.). Fax: 81-92-5837787.

† Kyushu University.

‡ Tsinghua University.

(1) Holmes, S. M.; Girolami, G. S. *J. Am. Chem. Soc.* **1999**, *121*, 5593. Hatlevik, Ø.; Buschmann, W. E.; Zhang, J.; Manson, J. L.; Miller, J. S. *Adv. Mater.* **1999**, *11*, 914.

(2) Decurtins, S.; Pellaux, R.; Antorrena, G.; Palacio, F. *Coord. Chem. Rev.* **1999**, *190*−*192*, 841. Grusell, M.; Train, C.; Boubekeur, K.; Gredin, P.; Ovanesyan, N. *Coord. Chem. Rev.* **2006**, *250*, 2491. Clement, R.; Decurtins, S.; Gruselle, M.; Train, C. *Molecular magnets: Recent highlights*; Springer: New York, 2003; p 1. Pikington, M.; Decurtins, S. *Magnetism: molecules to materials II*; Wiley-VCH-Verlag GmbH: Weinheim, Germany, 2001; p 339.

(3) (a) Coronado, E.; Galan-Mascaros, J. R.; Gomez-Garcia, C. J.; Laukhin, V. *Nature* **2000**, *408*, 447. (b) Benard, S.; Riviere, E.; Yu, P.; Nakatani, K.; Delouis, J. F. *Chem. Mater.* **2001**, *13*, 159.

(4) (a) Goodwin, H. C. *Top. Curr. Chem.* **2004**, *234*, 23. (b) Gütlich, P.; Hauser, A.; Spiering, H. *Angew. Chem., Int. Ed. Engl.* **1994**, *33*, 2024. (c) Krivokapic, I.; Zerara, M.; Daku, M. L.; Vargas, A.; Enachescu, C.; Ambrus, C.; Tregenna-Piggott, F.; Amstutz, N.; Krausz, E.; Hauser, A. *Coord. Chem. Rev.* **2007**, *251*, 364.

(5) Murray, K. S.; Kepert, C. J. *Top. Curr. Chem.* **2004**, *233*, 195.

(6) Sieber, R.; Decurtins, S.; Stoeckli-Evans, H.; Wilson, C.; Yufit, D.; Howard, J. A. K.; Capelli, S. C.; Hauser, A. *Chem.—Eur. J.* **2000**, *6*, 361.

(7) Tiwary, S. K.; Vasudevan, S. *Inorg. Chem.* **1998**, *37*, 5239.

(8) Coronado, E.; Mascaros, J. R. G.; Gimenez-Lopez, M. C.; Almeida, M.; Waerenborgh, J. C. *Polyhedron* **2007**, *26*, 1838.

(9) Harris, C. M.; Lockyer, T. N.; Martin, R. L.; Patil, H. R. H.; Sinn, E.; Stewart, I. M. *Aust. J. Chem.* **1969**, *22*, 2105.

(10) Deep-red single crystals of **1** were obtained by slow diffusion of $[Co(terpy)_2]Cl_2$ in MeOH into an aqueous solution of $MnCl_2-K_3[Cr(ox)_3]$ (molar ratio Co:Mn:Cr = 1:2:1). **2** can only be obtained when Cl^- is absent. Therefore, excessive $Ag_3Cr(ox)_3$ was used to react with $MnCl_2\cdot 4H_2O$ in MeOH to completely remove Cl^-. Methanolic $[Co(terpy)_2]-I_2$ was employed instead of $[Co(terpy)_2]Cl_2$ to diffuse slowly to the above $Mn^{II}Cr^{III}(ox)_3$ mixture, giving light-red single crystals. Elem anal. Calcd for $C_{36.5}H_{28}ClCoCrMnN_6O_{14.5}$ (**1**): C, 44.55; H, 2.87; N, 8.54. Found: C, 44.03; H, 2.80; N, 8.82. Calcd for $C_{42.5}H_{38}CoCr_2Mn_2N_6O_{31.5}$ (**2**): C, 36.21; H, 2.72; N, 5.96. Found: C, 36.03; H, 2.85; N, 6.02. IR (KBr): 1629 and 1683 cm^{-1} for **1**; 1631 and 1672 cm^{-1} for **2**.

10.1021/ic701043f CCC: $37.00
Published on Web 10/20/2007

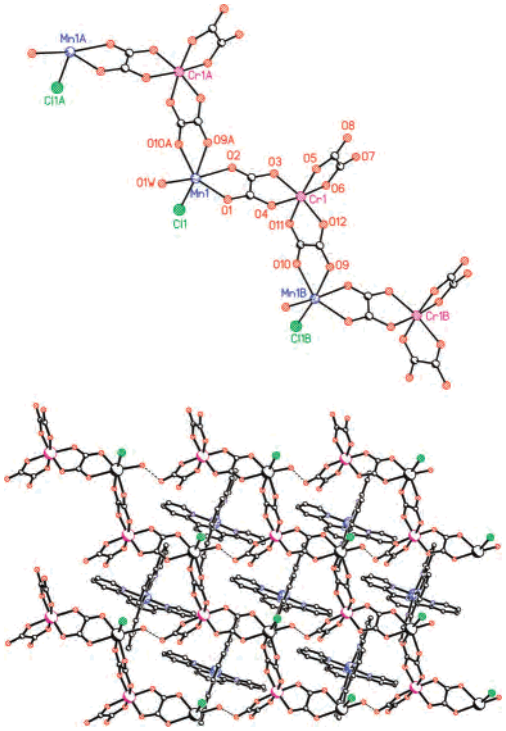

Figure 1. Top: structure of the oxalate-bridged anionic chain of complex **1**. Bottom: hydrogen-bonded layer with $[Co(terpy)_2]^{2+}$ in the vicinity of the layer.

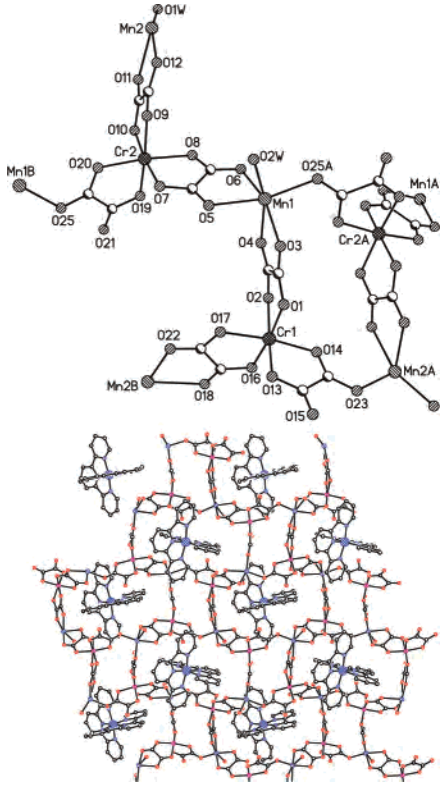

Figure 2. Top: connection modes of the Mn^{II} and Cr^{III} ions in **2**. Bottom: layered structure of **2** along the *c* axis.

($T_{1/2}$) of ca. 200 K, whereas the transition moves to higher temperatures when the anion is small; e.g., for $[Co(terpy)_2]Cl_2$, $T_{1/2}$ is greater than 300 K.[9]

The molecular structures[11] of complexes **1** and **2** are shown in Figures 1 and 2, respectively. The structure of **1** consists of a new 1D $[Mn(H_2O)Cl(ox)Cr(ox)_2]^{2-}$ anionic chain and a $[Co(terpy)_2]^{2+}$ cation. The anionic chain contains alternating $[Mn(H_2O)Cl]^{+}$ and $[Cr(ox)_3]^{3-}$ connected by two oxalate ligands of $[Cr(ox)_3]^{3-}$. The Mn^{2+} is linked with one Cl^{-} anion and five O atoms from two chelating ox^{2-} bridges and one coordinating water atom. The Mn−O bond distances range from 2.160(7) to 2.341(7) Å, and the Mn−Cl bond distance is a little longer, 2.373(3) Å. As usual, the Cr^{3+} is coordinated by six O atoms from three oxalate ligands, with the Cr−O bond distances ranging from 1.935(6) to 2.007(6) Å. The oxalate-bridged 1D chains are hydrogen-bonded through the nonbridging oxalate O atoms and the coordinating water O atoms of adjacent chains, giving rise to a hydrogen-bonded layer (Figure 1, bottom). The $[Co(terpy)_2]^{2+}$ cations are positioned between the layers (see Figure 1 and the Supporting Information).

The structure of complex **2** consists of a 2D oxalate-bridged layer $[Mn(H_2O)Cr(ox)_3]_n^{n-}$ and a charge-balancing $[Co(terpy)_2]^{2+}$ cation. The 2D anionic layer contains two unique (albeit similar) Mn or two independent Cr ions connected by oxalate ligands (Figure 2). The Cr ion is coordinated by six O atoms of three oxalate ligands, while the Mn ion is linked to six O atoms of two bidentate oxalate ligands, a monodentate oxalate ligand, and a water molecule. The Mn−O bond distances are in the range of 2.210(7)−2.365(9) Å. The layer consists of two different nets, large Mn_4Cr_4 rectangles and small Mn_2Cr_2 rectangles (Figure 2, bottom). The previously reported 2D oxalate-bridged anionic layers have the common planar honeycomb structure, and complex **2** has a unique 2D structure motif among oxalate-bridged bimetallic species. The layers are not planar but corrugated, and $[Co(terpy)_2]^{2+}$ cations are accommodated in the hollow of the layer and are partly embedded within the large rectangles (see the Supporting Information).

The Co−N bond distances in the $[Co(terpy)_2]^{2+}$ cation range from 1.895(7) to 2.117(9) Å for **1** (173 K) and from 1.853(14) to 1.971(14) Å for **2** (113 K), corresponding to low-spin Co^{II} at the temperatures. The Co−N bond distances in low-spin $[Co(terpy)_2]^{2+}$ have been shown to be in the range of 1.912−2.083 Å.[4a]

Variable-temperature direct current magnetic susceptibility data were collected on a bundle of crystals from 5 to 300 K (Figures 3 and 4 for complexes **1** and **2**, respectively). The room-temperature $\chi_m T$ value (7.02 emu K mol^{-1}) at 300 K for **1** is slightly higher than the expected spin-only value (6.625 emu K mol^{-1}) for one Mn^{II} ion ($S = 5/2$), one Cr^{III} ion ($S = 3/2$), and one low-spin Co^{II} ion ($S = 1/2$). With a decrease of the temperature, the $\chi_m T$ value slightly decreases and reaches a minimum value of 6.98 emu K mol^{-1} at 260 K. Below 260 K, the $\chi_m T$ value increases, reaching a value of 15.77 emu K mol^{-1} at 5 K. This behavior indicates the

(11) Crystal structure data for **1**: $C_{36.5}H_{28}ClCoCrMnN_6O_{14.5}$ ($M_r = 983.97$), monoclinic, *Cc*, $a = 12.991(3)$ Å, $b = 12.200(2)$ Å, $c = 25.812(5)$ Å, $\gamma = 101.63(3)°$, $V = 4006.7(14)$ Å^3, $T = 173$ K. R1 = 0.0695, wR2 = 0.1131 [$I > 2\sigma(I)$], and $S = 1.045$. Crystal structure data for **2**: $C_{42.5}H_{38}CoCr_2Mn_2N_6O_{31.5}$ ($M_r = 1409.60$), monoclinic, $P2_1/n$, $a = 14.693(3)$ Å, $b = 17.947(4)$ Å, $c = 20.005(5)$ Å, $\gamma = 98.2571(13)°$, $V = 5220(2)$ Å^3, $T = 113$ K. R1 = 0.1125, wR2 = 0.2188 [$I > 2\sigma(I)$], and $S = 1.084$.

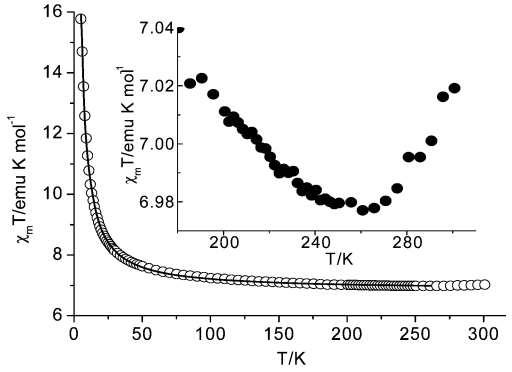

Figure 3. Temperature dependence of $\chi_m T$ for **1** in an applied field of 2 kOe. The solid line represents the best fit. Inset: enlarged view in the temperature range of 180−300 K.

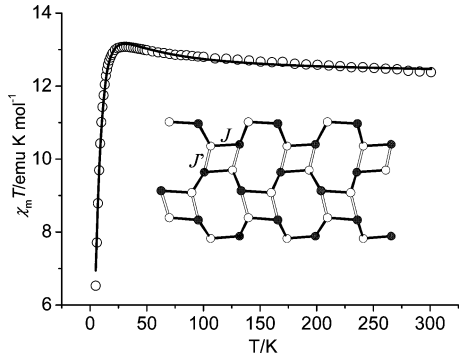

Figure 4. Temperature dependence of $\chi_m T$ for **2** in an applied field of 2 kOe. The solid line represents the best fit. Inset: model for the fitting ($J \gg |J'|$). Oxalate bridges have been shown by straight rods: solid, bis(bidentate) bridges; hollow, bidentate/monodentate bridges.

presence of dominant ferromagnetic interactions between Mn^{II} and Cr^{III}, which is usual for bidentately oxalate-bridged $Mn^{II}-Cr^{III}(ox)_3$ systems.[3,12−14]

Considering the incorporation of a possible SCO $[Co(terpy)_2]^{2+}$ cation, the slight increase of $\chi_m T$ from 260 to 300 K most likely originates from the spin transition of $[Co(terpy)_2]^{2+}$. To eliminate the effect of solvents, magnetic susceptibility measurements have been performed from 320 to 2 K. An increase of $\chi_m T$ from 260 to 320 K exists (see the Supporting Information), which should be assigned to spin transition rather than the solvent effect.

The magnetic susceptibility of complex **1** can be fitted to the equation (see the Supporting Information) based on the Hamiltonian $\hat{H} = -\sum_{i=0}^{N} J\hat{S}_i\hat{S}'_{i+1}$ suitable for the 1D Heisenberg alternating spin systems.[13] The contribution of $[Co(terpy)_2]^{2+}$ was considered as constant in the form of $\chi_m T = Ng^2\beta^2 S(S+1)/3k$, where $S = {}^1/_2$ for low-spin Co^{II}.[4c] The fit to the magnetic data in the temperature range of 5−260 K gave the parameters $J = 1.18(1)$ cm^{-1}, $g = g_{Mn} = g_{Cr} = g_{Co} = 2.03(1)$, and $zJ' = -0.038(1)$ cm^{-1}. The inclusion of zJ' accounts for the interchain magnetic coupling.

The magnetic susceptibility of complex **2** is a little different. Although a similar global ferromagnetic interaction is present, the absence of a minimum in the $\chi_m T-T$ curve suggests no spin transition of $[Co(terpy)_2]^{2+}$ (Figure 4). The room-temperature $\chi_m T$ value of 12.4 emu K mol^{-1} is consistent with the spin-only theoretical value of 12.875 emu K mol^{-1} assuming that Co^{II} is low-spin.

Alternatively, the layer (Figure 2, bottom) can be regarded as bidentate oxalated-bridged (toward Mn) $Mn^{II}-Cr^{III}$ chains linked by monodentate oxalate bridges (toward Mn), as illustrated in the inset of Figure 4. From the magnetic viewpoint, the former pathway usually transmits a ferromagnetic $Mn^{II}-Cr^{III}$ coupling while the latter transfers an antiferromagnetic $Mn^{II}-Cr^{III}$ interaction.[15] Considering that the former is much stronger than the latter,[14] the oxalate-bridged layer can be thought of as weakly antiferromagnetically coupled chains. Therefore, a mean-field approach[16] (see the Supporting Information) can be used with the model shown in the inset of Figure 4. The best fit to the magnetic susceptibilities of **2** in the whole temperature range gave the parameters $J = 2.47(1)$ cm^{-1}, $g = g_{Mn} = g_{Cr} = g_{Co} = 2.03(1)$, and $zJ' = -0.35(1)$ cm^{-1}. The J values for complexes **1** and **2** are close to those for bis(bidentate) oxalate-bridged $Mn^{II}-Cr^{III}$ complexes.[12−14] Field-cooled magnetization (FCM) of **2** shows the absence of 3D magnetic ordering down to 2 K possibly because of the presence of monodentate oxalate bridges in the 2D layer.

In summary, we have shown that the SCO $[Co(terpy)_2]^{2+}$ cation can be integrated in oxalate-bridged $Mn^{II}-Cr^{III}(ox)_3$ polymeric anions. The SCO behavior of $[Co(terpy)_2]^{2+}$ strongly depends on the chemical pressure of the polymeric anions: the transition moves to higher temperature when the $[Co(terpy)_2]^{2+}$ cation is incorporated between coordination bond-connected layers. This indicates that a hydrogen-bonded layered network gives weaker chemical pressure compared with the strong coordination bond-connected 2D network. A novel oxalate-bridged bimetallic 2D layer and a 1D chain structure are formed in the presence of the $[Co(terpy)_2]^{2+}$ cation. Further studies on the synthesis of analogues taking advantage of the chemical pressure to tune the SCO behavior are in progress.

Acknowledgment. The authors acknowledge the financial support of the Fok Ying Tong Education Foundation and a JSPS foundation.

Supporting Information Available: Cell packing diagrams of **1** and **2**, FCM plots for **1** and **2**, $\chi_m T-T$ plot measured from 320 to 2 K, magnetic fitting equations, and an X-ray crystallographic file in CIF format. This material is available free of charge via the Internet at http://pubs.acs.org.

IC701043F

(12) Coronado, E.; Galan-Mascaros, J. R.; Gimenez-Saiz, C.; Gomez-Garcia, C. J.; Ruiz-Perez, C.; Triki, S. *Adv. Mater.* **1996**, *8*, 737. Coronado, E.; Galan-Mascaros, J. R.; Gimenez-Saiz, C.; Gomez-Garcia, C. J.; Ruiz-Perez, C. *Eur. J. Inorg. Chem.* **2003**, 2290. Sun, Y.-Q.; Zhang, J.; Yang, G.-Y. *Dalton Trans.* **2006**, 1685.

(13) Coronado, E.; Galan-Mascaros, J. R.; Gomez-Garcia, C. J.; Marti-Gastaldo, C. *Inorg. Chem.* **2005**, *44*, 6197.

(14) Alberola, A.; Coronado, E.; Gimenez-Saiz, C.; Gomez-Garcia, C. J.; Romero, F. M.; Tarazon, A. *Eur. J. Inorg. Chem.* **2005**, 389. Ballester, G.; Coronado, E.; Gimenez-Saiz, C.; Romero, F. M. *Angew. Chem., Int. Ed.* **2001**, *40*, 792.

(15) Marinescu, G.; Visinescu, D.; Cueos, A.; Andruh, M.; Journaux, Y.; Kravtsov, V.; Simonov, Y. A.; Lipkowski, J. *Eur. J. Inorg. Chem.* **2004**, 2914. Marinescu, G.; Andruh, M.; Lescouezec, R.; Munoz, M. C.; Cano, J.; Lloret, F.; Julve, M. *New J. Chem.* **2000**, *24*, 527.

(16) Chiari, B.; Cinti, A.; Piovesana, O.; Zanazzi, P. F. *Inorg. Chem.* **1995**, *34*, 2652.